分子生物学 basic technique

その 31

細胞膜マイクロドメイン（ラフト）を免疫原とした抗体作成法

Monoclonal and polyclonal antibodies against lipid microdomain, raft

国立成育医療センター研究所発生・分化研究部
形態発生研究室室長
片桐　洋子

国立成育医療センター研究所発生・分化研究部
機能分化研究室室長
大喜多　肇

国立成育医療センター研究所副所長
藤本純一郎

国立成育医療センター研究所発生・分化研究部
部長
清河　信敬

はじめに

CD抗原に代表される初期の単クローン抗体は，細胞そのものを免疫原として得られたものが多い。水溶性の抗原物質にしろ細胞性の抗原にしろ，Freund's adjuvantと混合してエマルジョンにし，動物に免疫するのが常道である。筆者らは細胞膜のマイクロドメイン（ラフト）を免疫原とすることにより，adjuvantとの混合の必要もなく効果的に免疫応答を惹起することができた。ラフトを免疫原とする抗体産生法とその特性について述べる。

細胞膜はタンパクが埋め込まれた脂質二重層の2次元的な広がりであるが，決して均一なものではなく，糖脂質やスフィンゴミエリン，コレステロール，長鎖で飽和脂肪酸に富んだリン脂質がマイクロドメインを形成し，GPIアンカー型タンパク，Src型キナーゼ，Gタンパクなど，シグナル伝達に関わる分子がコンパクトに収まっている。マイクロドメインを大海に浮かぶ筏に例えたラフトという呼称は，ネーミングのよさも手伝って広く使われており，本稿でもラフトと呼ぶことにする。

Ⅰ．ラフトの調製

ラフトは界面活性剤不溶性の低密度膜画分として得られる。回収した細胞を，氷冷1％Triton可溶化バッファー［1％Triton X-100(v／v)／0.15M NaCl／25mM Tris-HCl buffer，pH 7.5／1 mM PMSF］で可溶化後，Dounce homogenizerで手動でホモジェナイズする。600rpm，5分の遠心分離で得られた上清に，85％ショ糖溶液［85％ショ糖（w／v)／0.15M NaCl／10mM Tris-HCl buffer，pH 7.5］を加えて40％ショ糖濃度に調整する。スイングローター用超遠心管の管底に40％ショ糖濃度ライゼートを入れ，30％ショ糖溶液，さらに5％ショ糖溶液を重層する。Beckman SW40Tiローター中で38,000rpm，16～18hr遠心の後，30％と5％ショ糖溶液の界面にラフト画分が肉眼で観察される。ラフトを回収し

てPBSで希釈し，小型冷却遠心機15,000rpm，30分の遠心で沈殿する。PBSによる洗浄を3回繰り返し，ショ糖を除く。ヒト腎癌細胞株ACHN細胞の場合，10cmプレート5枚から12μgタンパク，183μg脂質のラフトが得られる。

Ⅱ．単クローン抗体の作成

ラフトのPBS懸濁液をBalb/cマウスの皮下に注射する。1回の免疫には5～10μgタンパク，1～5×10^7個細胞からのラフトが目安となる。5～7日の間隔をおいて4回の追加免疫の後，抗体価の上昇をフローサイトメトリーで確認する。抗体価の上昇が確認されたら，常法に則りミエローマと融合させてハイブリドーマを作成し，HAT／10%牛胎児血清含有RPMI培地中でコロニーが出てくるまで培養を続ける。スクリーニングはフローサイトメトリーが最も確実であるが，細胞内の分子を認識していることもありうるので，固定後サポニンなど(BD Cytofix/Cytoperm, BD Biosciences)で細胞膜に穴をあけ解析する必要がある。筆者らはドットブロット免疫染色法でtime & money savingにスクリーニングしている。50～100ng protein／50μL／ドットのラフトをドットブロッターでPVDF膜にブロットし，各ドットを撥水性のペン(DAKO PEN)で仕切る。5%スキムミルクでブロック後，湿箱内でハイブリドーマコロニーの培養上清10μLを各ドットにのせ室温で2時間静置する。これ以降は通常のWestern解析と同様である。一度に最大96クローンが検定でき，ランニングコストはきわめて安価で感度も高い。脂質認識性のクローンのスクリーニングは，ラフトのクロロフォルム／メタノール，2：1(v/v)(CM)抽出物を乾いた状態のPVDF膜に直接ドットブロットすればよい。筆者らはACHN細胞のラフトを免疫して，ドットブロット免疫染色法，細胞表面および細胞内染色のフローサイトメトリーを組み合わせて，①細胞表面のタンパクを認識するのが7クローン，②細胞膜の内側のタンパクを認識するのが3クローン，③細胞表面の脂質を認識するのが21クローン得られた[1]。

Ⅲ．抗ACHN細胞ラフト単クローン抗体Raft.1とRaft.2の認識抗原

ラフトを介するシグナル伝達機構の解明を目的として単クローン抗体作りを始めたので，細胞の内側にあって刺激に伴い細胞内分布が大きく変化するクローンをスクリーニングしたところ，未刺激ACHN細胞では細胞膜の細胞質側が均一に染色されるが，刺激後30分のACHN細胞では核近辺に収束した形で染色されるクローンRaft.1が得られた[2]。抗原解析の結果，Raft.1はGタンパクβ1～4鎖を認識抗原としていることが確認された。Gタンパクβ1～4鎖は種を超えてきわめて高度に保存された分子なので抗体作りは困難であるといわれていたが，ラフト免疫法だと可能である。

ACHN細胞ラフトは重量比で90%が脂質であるからか，3分の2が脂質反応性のクローンであった。そのうちの1つを再クローニングして得られたRaft.2はグロボ系スフィンゴ糖脂質のsialylGb5(SSEA－4抗原エピトープ)を認識する。しかしながら，他の20クローンもsialylGb5のみを認識抗原としていた(図1)。タンパク性のSSEA-4糖鎖にも反応し[3]，従来の抗体とは違ったユニークな認識エピトープを有していると考えられる。

Ⅳ．抗ラフト抗血清

上記ACHNラフト免疫マウスのハイブリドーマ作成直前に採取した血清のTLC免疫染色像はsialylGb5のみに反応しており，monospecificな抗糖脂質抗体ができていたことを示している。ACHN細胞はグルコシルセラミド(GlcCer)以下sialylGb5までグロボ系糖脂質がほぼ均等に発現しており，sialylGb5がとりわけ多いわけではない。ACHN細胞のみにみられる現象かどうかを検証するため，他の細胞ラフトでも試してみたところ，ヒト異形大細胞型リンパ腫細胞株Karpas,

サル腎由来細胞株Vero細胞，マウスT白血病細胞株EL4で同様の現象がみられた(図2左)。すなわち，ラフトのPBS懸濁液を皮下に注入するだけで，得られた抗血清はmonospecificなポリクローナル抗体となる。一方，放射線照射したEL4細胞やVero細胞，Karpas細胞を皮下注入しても糖脂質に対するmonospecificな抗血清は得られなかった。C57BL/6にACHN細胞やEL4細胞のラフトを免疫しても全く同様の結果が得られ，Balb/cマウスに限ったことではないこともわかった。EL4細胞はC57BL/6由来の細胞であるので，EL4細胞ラフトに対して起きるC57BL/6マウスの抗体産生反応は自己免疫反応の可能性もあるが，抗DNA抗体の上昇はみられなかった。ラフト免疫で血清内に産生される抗体の出現パターンを調べてみると，IgMの出現に始まり，やがてIgMに代わってIgGが出現するという典型的なT-B共役型の抗体産生反応であった(図2右)。

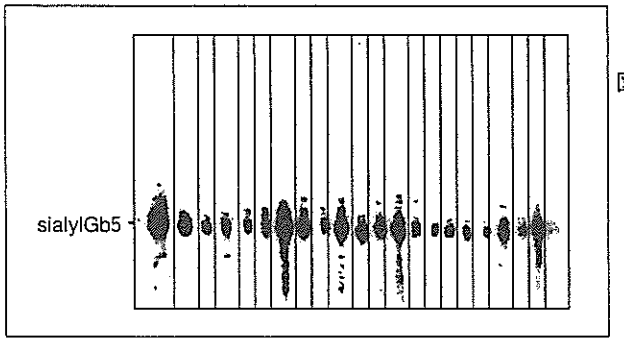

図1．抗ACHNラフト単クローン抗体脂質反応性クローンのTLC免疫染色
ACHN細胞ラフトの脂質分画をHPTLCプレートの原点に直線状にスポットしてTLC展開し，PVDF膜にブロット後22本のストリップに切り離した。各ストリップを脂質反応性クローンの培養上清／HRP標識ウサギ抗マウスIgG+M抗体でプロービングし，ECL (Amersham Biosciences)で可視化した。すべてのクローンがsialylGb5と反応しているのがわかる。

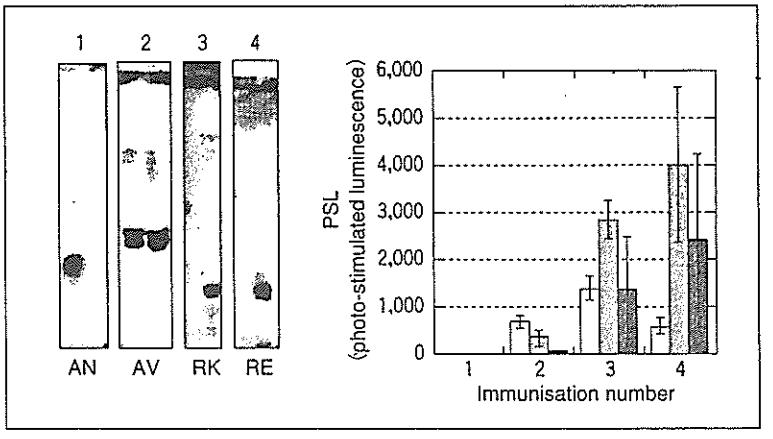

図2．抗ラフト抗血清のTLC免疫染色と，抗体価の経時変化
左：ACHN細胞(1)，Vero細胞(2)，Karpas細胞(3)，EL4細胞(4)ラフトに対する抗血清のTLC免疫染色。ACHN(A)，Nalm16(N)，Vero(V)，EL4(E)細胞の脂質分画と標準糖脂質(R：GD3, GD1a, GD1b, 各1 μg)をTLC展開後，polyisobutyl methacrylateでコートし抗血清で免疫染色した。いずれの抗血清も単一の糖脂質と反応している。展開溶媒：C/M/0.2%$CaCl_2$＝60：35：8(1)，5：4：1(2～4)。
右：抗ACHN脂質抗体の経時変化。ACHN細胞ラフトで免疫したマウスの血清を各免疫1週間後に採取し，ドットブロット免疫染色法で抗脂質抗体価をIgM型(□)，IgG型(□)別に解析した。定量はECL発色後，LAS-1000(Fuji film)で行った。sialylGb5(■)に対する抗体価の検定は，TLC免疫染色後にLAS-1000で定量した。

おわりに

以上ラフトを免疫原とすることの利点について，ヒトACHN細胞のラフトを免疫原とした筆者らの例を中心に概説した。実験当初adjuvantが不要かどうか不明であったので，adjuvant添加，非添加で同時に免疫，細胞融合したところ，前者でコロニー出現が早かった点以外に，全く両者に違いはなかった。ラフト調製の際のdetergentの濃度，種類によりラフトに回収されるタンパクは異なる。他のオルガネラやラフト以外のタンパクの混入は避けられなく，それが重要な意味をもっていることもあるので，慎重な判断を要する。また，すべての細胞のラフトでmonospecificな抗糖脂質抗血清が得られるわけではなく，どの糖脂質が抗原として選択されるのか，その規則性は不明である。実際にやってみないとわからないのが現状であるが，シアリル化された五糖以上の糖脂質が抗原になりやすいようである。さまざまな細胞由来のラフト免疫に関するデータの蓄積が待たれる。

文　献

1）Katagiri YU, Ohmi K, Katagiri C, et al : Prominent immunogenicity of monosialosyl galactosylgloboside, carrying a stage-specific embryonic antigen-4 (SSEA-4) epitope in the ACHN human renal tubular cell line-a simple method for producing monoclonal antibodies against detergent-insoluble microdomains/raft. Glycoconj J 18 : 347-353, 2001

2）Katagiri YU, Ohmi K, Tang W, et al : Raft. 1, a monoclonal antibody raised against the raft microdomain, recognizes G-protein β 1 and 2, which assemble near nucleus after Shiga toxin binding to human renal cell line. Lab Invest 82 : 1735-1745, 2002

3）Katagiri YU, Kiyokawa N, Nakamura K, et al : Laminin binding protein, 34/67 laminin receptor, carries stage-specific embryonic antigen-4 epitope defined by monoclonal antibody Raft.2. Biochem Biophys Res Commun 332 : 1004-1011, 2005

その 32

酵母の遺伝学（出芽酵母・分裂酵母）

The genetics of yeast (budding yeast & fission yeast)

大阪大学大学院医学系研究科
生体制御医学・生化学

田邊　香

はじめに

出芽酵母（*Saccharomyces cerevisiae*）と分裂酵母（*Schizosaccharomyces pombe*）は，細胞周期，情報伝達や代謝制御などの真核細胞の基礎的研究のモデル生物として，あるいはツールとしてよく利用されている。

酵母に共通する利点として，細胞周期が約3時間と短いため実験にかかる時間もまた比較的短くて済むこと，また遺伝子破壊や遺伝子導入などの分子遺伝学的，分子生物学的手法が確立されていて比較的容易であることが挙げられる。そこで，基本的な分子機構・現象を酵母で調べてから高等生物の系で確認する，といったケースが少なくない。

また，どちらも“酵母”でありながら，これら2つの生物種は系統樹上で遠く離れており，“出芽酵母と分裂酵母”は“出芽酵母とヒト”と同じくらい離れているともいわれている。両酵母にあてはまる現象は動物にもあてはまるとする立場さえある。遺伝子操作を行う上でほぼ同程度の容易さ，利点をもつこれら2つの酵母をお互いに足りないものを補い合うべく平行して研究することによって，真核細胞のもつ一般的，普遍的な性質の解明につながる重要な知見が得られることが期待されている。

BRIEF REPORT
Ewing Sarcoma/Primitive Neuroectodermal Tumor of the Kidney in a Child

Miho Maeda, MD,[1]* Akio Tsuda, MD,[1] Shingo Yamanishi, MD,[1] Yoko Uchikoba, MD,[1] Yoshitaka Fukunaga, MD,[1] Hajime Okita, MD,[2] and Jun-ichi Hata, MD[3]

A 6-year-old female was admitted with abdominal pain and a mass in the right abdomen. Her lactose dehydrogenase level was 1,200 IU/L, and neuron specific enolase was 120 ng/ml. Computed tomography scan confirmed a large right renal mass with necrosis. A right radical nephrectomy was performed. The tumor was completely encapsulated. Based on small round cell histology, strong MIC-2 (CD99) positive tumor cells, and EWS-FLI-1 fusion transcript, Ewing sarcoma/primitive neuroectodermal tumor of the kidney was diagnosed. Induction and follow-up with seven cycles of chemotherapy were given after surgery. She has had no evidence of recurrence 90 months from diagnosis. Pediatr Blood Cancer

Key words: electron microscopy; Ewing sarcoma/primitive neuroectodermal tumor; EWS-FLI-1; immunohistochemistry; kidney

INTRODUCTION

Ewing sarcoma/primitive neuroectodermal tumor (ES/PNET) of the kidney is a rare and highly malignant neoplasm. It affects young adults, and only a few pediatric cases (younger than 15 years) have been reported [1–9]. ES/PNET arising in the kidney act aggressively and show poor response to therapy [1]. ES/PNET of the kidney needs to be differentiated from other small round cell tumors of the kidney, because each type of tumor is treated differently. The diagnosis of this neoplasm is currently based on a combination of light microscopy, immunohistochemistry, electron microscopy, chromosomal analyses, and specific chimeric transcripts. Our patient, who was diagnosed by histochemistry and molecular biology analysis of the resected kidney and treated with chemotherapy, has remained alive more than 90 months after diagnosis.

CASE

A 6-year-old female was admitted to our hospital with abdominal pain and an abdominal mass. On physical examination, a large and firm mass was evident in the right abdomen. Laboratory evaluation showed a lactate dehydrogenase level of 1,200 IU/L (normal 218–411 IU/L), a neuron specific enolase level of 120 ng/ml (normal <10 ng/ml), and ferritin level of 160 ng/ml (normal 15–89 ng/ml). Urine catecholamine levels were within normal limits. Abdominal computed tomography (CT) scan confirmed a large right renal mass with areas of necrosis and bleeding. There was no obvious lymphadenopathy and no intra-abdominal metastasis. Bone scintigraphy and CT scan of the thorax did not detect metastasis.

A right radical nephrectomy was performed. The tumor involved a large portion of the lower part of the kidney. The tumor was completely encapsulated and was 5.0 × 4.5 × 4.5 cm. Lymph nodes were negative for malignancy. Histologic examination revealed a small round cell tumor with massive necrosis, but no rosette formations. Periodic acid-Schiff (PAS) staining revealed diastase sensitive material in the tumor cell cytoplasm. Immunohistochemistry revealed that tumor cells were strongly positive for MIC-2 (CD99) as well as vimentin. The tumor cells were negative for chromogranin A, neurofilament, and synaptophysin. Electron microscopic examination showed a high nuclear-cytoplasm ratio and aggregated glycogen granules in the cytoplasm (Fig. 1A). A higher magnification of tumor cells showed neurosecretory-type granules, microtubules, and desmosome-like structures (Fig. 1B). The expression of EWS-FLI-1 fusion transcript was demonstrated by molecular biology (Fig. 2). A single 330 base pair cDNA product was detected by ethidium bromide staining, corresponding to the EWS-FLI-1 as previously reported by Sorensen et al. [10]. Direct DNA sequencing confirmed the presence of a fusion of EWS exon 7 to the FLI-1 exon 6. Unfortunately chromosomal findings failed because proliferation of the tumor cells was poor. According to results on small round cell histology and immunohistochemical profiles, electron microscopic findings, and EWS-FLI-1 fusion transcript, the tumor was diagnosed as an ES/PNET of the kidney. Therapy was initiated with 1.5 gm/m^2 vincristine on days 1, 8, 15, 22, 29, and 36; 500 mg/m^2 cyclophosphamide on days 2, 9, 30, and 37; and 0.45 mg/m^2 dactinomycin on days 16–20 for induction and then a total of seven cycles of 4-drug chemotherapy, consisting of 1.5 gm/m^2 vincristine on days 1, 15, 22, 29, 36, and 43; 0.45 mg/m^2 dactinomycin on days

[1]Department of Pediatrics, Nippon Medical School, Tokyo, Japan; [2]Department of Developmental Biology, National Research Institute for Child Health and Development, Tokyo, Japan; [3]Department of Pathology, National Center for Child Health and Development, Tokyo, Japan

*Correspondence to: Miho Maeda, 1-1-5 Sendagi, Bunkyo-ku, Tokyo 113-8603, Japan. E-mail: maeda@nms.ac.jp

Received 6 January 2006; Accepted 9 February 2006

DOI 10.1002/pbc.20831

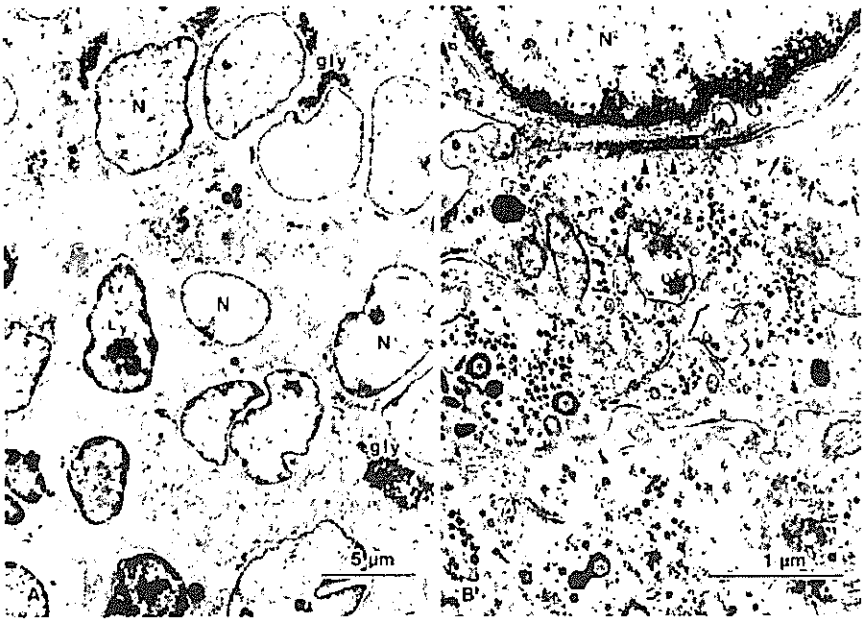

Fig. 1. Ultrastructural findings in the tumor cells. **A**: Tumor cells are oval and small (about 8–10 μm in a diameter). Nuclear-cytoplasm ratio is high. Nucleus has a few heterochromatin. Aggregated glycogen granules (gly) are observed in the cytoplasm. Ly, lymphocytes; N, nuclei. **B**: Neurosecretory granules (asterisks), microtubules (arrows), and desmosome-like structures (arrowheads) are observed in the tumor cells under higher magnification.

1–5; 500 mg/m^2 cyclophosphamide on days 16, 23, 30, 37, and 44; and 60 mg/m^2 doxorubicin on day 44 after surgery. She had no serious adverse effects during chemotherapy. She had no evidence of recurrence after 90 months from diagnosis and no late effects have been noted.

DISCUSSION

Though the existence of renal PNET was reported in 1975 in a review of pediatric PNETs [11], only a small number of cases have been reported. Recently, Parham et al. [12] from National Wilms Tumor Study Group Pathology Center reported that 79 of 146 cases of primary malignant neuroepithelial tumors of the kidney in adults and children were considered to be ES/PNET. Follow-up information, however, was only provided for 14 of 146 cases, and it is unclear which, if any, of those were actually ES/PNET [8]. Pediatric cases (younger than 15 years old) of ES/PNET of the kidney are extremely rare, and only ten cases have been reported previously [1–9]. Clinical characteristics, pathologic features, treatments, and outcomes of those cases are summarized in Table I.

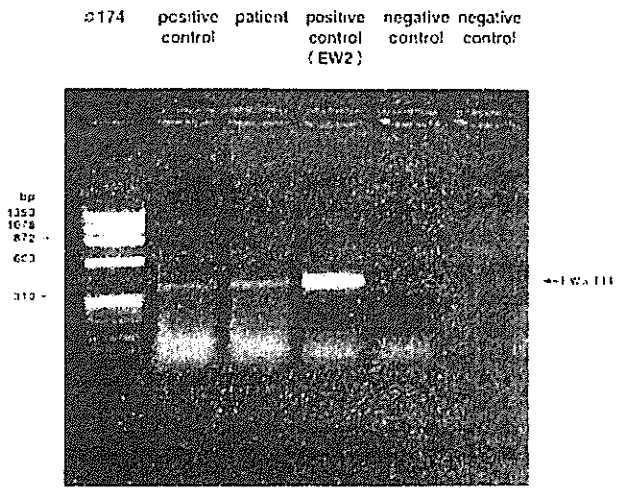

Fig. 2. A single 330 base pair transcript is detected in the patient sample following reserve transcriptase polymerase chain reactor (RT-PCR) performed on RNA extract from tumor tissue.

Several approaches can be used to arrive at a diagnosis of ES/PNET. The first approach is light microscopic examination of tumor tissue including immunohistochemistry. These tumors consist of primitive-appearing round cells with high nucleus to cytoplasmic ratios. The immunohistochemical features of ES/PNET are positive for CD99 (MIC2); however, expression of CD99 is by no means specific for ES/PNET among round cell tumors [13]. Although FLI-1 is a variable histochemical marker for ES/PNET, it is also positive in lymphoblastic lymphoma [14]. In contrast, WT-1 is a positive marker of Wilms tumor and desmoplastic round cell tumors, whereas it is a negative marker for ES/PNET, neuroblastoma and rhabdomyosarcoma. The second approach is electron microscopic examination of tumor tissue. Electron microscopic features include a specific high nuclear-cytoplasm ratio and aggregated glycogen granules in the cytoplasm. Neural differentiation appears on some cells with polar processes, which may contain microtubules or

TABLE I. Clinical and Pathological Features of ES/PNET of the Kidney in Pediatric Cases

Case	Ref.	Age	Gender (yr)	Symptoms	Metastasis	Pathology (immunohistochemistries)	Chimeric transcript	Therapy	Outcome (follow-up [Mo])
1	1	4	F	Abdominal pain, fever	RPLN, liver	CD99(+),NSE(+),S-100(+), Ker(+),Act(−),Vim(−),Chro(−)	NS	IFO, CBP, VP-16 radiation	Died (1)
2	1	14	M	Bone pain, weight loss	Lung, bone, bone marrow	CD99(+),NSE(+),Vim(+),Synapto(+) (±)S-100(−),Ker(−),Act(−),Chro(−)	EWS/FLI-1(−) EWS/ERG(−)	CY, VCR, DOX,IFO,VP-16 auto BMT	Alive (under treatment)
3	2	13	NS	Abdominal pain, hematuria	No	MIC2(+),NSE(+),Ker(−),Des(−), Act(−)	EWS/FLI-1(+)	Nephrectomy chemotherapy	NS
4	3	10	M	Abdominal mass	No	MIC2(+),NSE(+),Leu7(+), S-100(−),Ker(−), Des(−),Vim(−),Chro(−)	EWS/FLI-1(+)	Nephrectomy chemotherapy	Alive (6)
5	4	5	F	NS	IVC, right heart	NS	NS		NS
6	5	15	F	Abdominal pain, abdominal distention	No	MIC2(+),Vim(+),NSE(−), S-100(−)	NS	Nephrectomy CY, VCR, DOX,IFO,VP-16	Alive (8)
7	6	9	M	Abdominal pain, abdominal mass, weight loss	No	MIC2(+),NSE(−),Vim(−),Ker(−), LCA(−)	NS	Nephrectomy CY, VCR, DOX,IFO,VP-16	Alive (relapse+) (10)
8	7	9	F	Abdominal distention, abdominal mass	No	CD99(+),LCA(−),Ker(−),Act(−), NFM(−)	EWS/FLI-1(+)	Nephrectomy IFO,VP-16,CY,DOX,VCR auto BMT	Died (5)
9	8	11	M	Gross hematuria, abdominal mass	No	CD99(+)	NS	Nephrectomy VCR, DOX, VP-16, CY, DAC	Alive (64)
10	9	14	F	Abdominal pain, abdominal mass	IVC, right heart, liver	NS	NS	Chemotherapy	Died (24)
11	Present case	6	F	Abdominal pain, abdominal mass	No	MIC2(+),Vim(+)NFM(−),Chrom(−)	EWS/FLI-1(+)	Nephrectomy VCR, DAC, CY, DOX.	Alive (90)

RPLN, retroperitoneal lymphonode; IVS, inferior vena cava; NSE, neuron specific enolase; Ker, keratin; Act, actin; Vim, Vimentin; Chro, chromogrn A; MIC2, B microgloblin; Des, desmin; NFM, neurofibrofilament; Synapto, sinaptophilin; IFO, ifomide; CBD, carboplatinum; CY, cyclophosphamide; VCR, vincristine; DOX, doxrubicine; DAC, actinomycin D; BMT, bone marrow transplantation.

neurosecretory glands [15]. The third approach is chromosomal translocation, such as t(11;22) (q24;q12) which is positive in 88–95% of ES/PNET cases [16]. The final approach involves a molecular biologic examination. In 90–95% of cases of ES/PNET, the chimeric transcript is EWS-FLI-1; the remaining 5–10% are EWS-ERG. Other transcripts, including EWS-ETV1 and EWS-EIAF, have also been reported [16].

In terms of prognosis, the 5-year disease-free survival rate of ES/PNET is 45–55% [17], but the prognosis of ES/PNET of the kidney appears worse [1,18]. In pediatric cases (Table I), 5 of 8 patients were alive when the cases were reported; however, 1 patient (no. 6) was alive with disease, 2 patients (no. 3 and no. 5) were followed-up only for 6 and 8 months, and 1 patient was under treatment (no. 9). The follow-up duration was not described in this case. Only 2 patients (no. 8 and our case) were alive after 5 years. For 2 patients, it was not defined whether they were alive or not (Table I). Jimenez et al. [8] described that 3 of 11 patients were alive for 4–64 months, and 5 patients had local recurrence or distance metastasis then died of their disease, and 3 patients were lost to follow-up. Most of the recent therapeutic protocol for children with ES/PNET consists of vincristine, doxorubicin, cyclophsphamide, ifosphamide, and etoposide. Radiation and surgery have been used; some patients have been treated with myeloablative chemoradiotherapy followed by autologous bone marrow rescue. In spite of a lack of radiation therapy and our not using ifosphamide and etoposide for chemotherapy, our patient has survived for a relatively long period with no recurrence. Possible reasons for this good outcome might include the pathologic features of the tumor, the well-encapsulated nature of the tumor with no involvement beyond the capsule and the accurate diagnosis followed by prompt treatment with chemotherapy. Several approaches including cytogenetical methods are important for early, accurate diagnosis of ES/PNET.

REFERENCES

1. Rodriguez-Galindo C, Marina NM, Fletcher BD, et al. Is primitive neuroectodermal tumor of he kidney a distinct entity? Cancer 1997;79:2243–2250.
2. Quezado M, Benjamin DR, Tsokos M. EWS/FLI-1 fusion transcripts in three peripheral primitive neuroectodermal tumors of the kidney. Hum Pathol 1997;28:767–771.
3. Takeuchi T, Iwasaki H, Ohjma Y, et al. Renal primitive neuroectodermal tumor: A morphologic, cytogenetic, and molecular analysis with the establishment of two cultured cell lines. Diag Mol Pathol 1997:6:309–317.
4. Hasanbegovic E, Terzic R, Sabanovic S, et al. Ewing's soft-tissue sarcoma-case report. Med Arh 1998;52:157–158.
5. Antoneli ABG, Coasta CML, de Camargo B, et al. Primitive neuroectodermal tumor (PNET)/extraosseous Ewing sarcoma of the kidney. Med Ped Oncol 1998;30:303–307.
6. Kuczynski AP, Gugelmin ES, Netto RAS. Primitive neuroectodermal tumor of the kidney in children. J Ped (Rio J) 2001;77:49–51.
7. Vicha A, Stejskalvo E, Sumerauer D, et al. Malignant peripheral primitive neuroectodermal tumor of the kidney. Cancer Genet Cytogenet 2002:139:67–70.
8. Jimenez RE, Folpe AL, Laspham RL, et al. Primitive Ewing's sarcoma/primitive neuroectodermal tumor of the kidney. Am J Surg Pathol 2002;26:320–327.
9. Ng AWH, Lee PSF, Howerd RG. Primitive neuroectodermal kidney tumor. Austral Radiol 2004;48:211–213.
10. Sorensen PHB, Liu XF, Delattre O, et al. Reverse transcriptase PCR amplification of EWS/FLI1 fusion transcripts as a diagnostic test for peripheral primitive neuroectodermal tumors of childhood. Diagn Mol Pathol 1993;2:147–157.
11. Seemayer TA, Thelmo WL, Bolande RP, et al. Peripheral neuroectodermal tumors. Perspect Pediatr Pathol 1975;2:151–172.
12. Parham DM, Roloson GJ, Feely M, et al. Primary malignant neuroepithelial tumors of the kidney. Am J Surg Pathol 2001:25:133–146.
13. Stevenson A, Chatten J, Bertoni F, et al. CD99 (p30/32MIC2) neuroectodermal/Ewing's sarcoma antigen as an immunohistochemical marker. Review of more than 600 tumors and literature experience. Appl Immunohistochemistry 1994;2:231–240.
14. Folpe AL, Hill CE, Parham DM, et al. Immunohistochemical detection of FLI-1 protein expression: A study of 132 round cell tumors with on CD99-positive mimics of Ewing's sarcoma/primitive neuroectodermal tumor. Am J Surg Pathol 2000;24: 1657–1662.
15. Suh CH, Ordonez NG, Hocks J, Mackay B. Ultrastracture of the Ewing's sarcoma family of tumor. Ultrastruct Pathol 2002;26:67–76.
16. Stephenson CF, Bridge JA, Sandberg AA. Cytogenetic and pathologic aspects of Ewing's sarcoma and neuroectodermal tumors. Human Pathol 1992;23:1270–1277.
17. Kushner BH, Hajdu SI, Gulati SC, et al. Extracranial primitive neuroectodermal tumors: The memorial Sloan-Kettering Cancer Center experience. Cancer 1991;67:1825–1829.
18. Benesch M, Urban C. Is primitive neuroectodermal tumor of the kidney a distinct entity? Cancer 1998:82:1414–1415.

Association of 11q Loss, Trisomy 12, and Possible 16q Loss with Loss of Imprinting of Insulin-Like Growth Factor–II in Wilms Tumor

Naoki Watanabe,[1,2] Hisaya Nakadate,[3] Masayuki Haruta,[1] Waka Sugawara,[1] Fumiaki Sasaki,[3] Yukiko Tsunematsu,[3] Atsushi Kikuta,[3] Masahiro Fukuzawa,[3] Hajime Okita,[3] Jun-ichi Hata,[3] Hidenobu Soejima,[4] and Yasuhiko Kaneko[1,3]*

[1]Research Institute for Clinical Oncology, Saitama Cancer Center, Ina, Saitama, Japan
[2]Department of Pediatrics, Juntendo University Nerima Hospital, Tokyo, Japan
[3]Japan Wilms Tumor Study Group, Tokyo, Japan
[4]Department of Biomolecular Sciences, Saga University, Saga, Japan

We evaluated the *WT1* and *IGF2* status and performed chromosome and/or comparative genomic hybridization analysis in 43 tumor samples from patients with Wilms tumor. On this basis, we classified them into 4 groups: *WT1* abnormality, loss of heterozygosity (LOH) of *IGF2*, loss of imprinting (LOI) of *IGF2*, and retention of imprinting (ROI) of *IGF2*, which were seen in 12%, 30%, 16%, and 42% of the tumors, respectively. Patients in the LOI group were older than those in other groups ($P < 0.01$), and tumors in the *WT1* group had fewer cytogenetic changes than did those in the other groups ($P < 0.01$). It was found that 11q− and +12 were more frequent in the LOI group than in the *WT1*+LOH+ROI group ($P < 0.01$ and $P < 0.01$). There was no difference in the incidence of 16q− between the LOI group and the other groups; however, when we excluded 16 tumors with LOH on 11p15, 16q− tended to be more frequent in the LOI group than in the *WT1*+ROI group ($P = 0.06$). The association of 11q− or +12 with LOI of *IGF2* found in the present study suggests that many tumors with no *WT1* abnormalities need overexpression of *IGF2* together with biallelic inactivation of the tumor-suppressor gene on 11q and/or overexpression of growth-promoting genes on chromosome 12. The 11q gene may code for one of the proteins that constitute a CTCF insulator complex, and its mutation, deletion, or haploinsufficiency may cause insulator abnormalities that might lead to LOI of *IGF2*.

INTRODUCTION

Wilms tumor is the most common kidney tumor in childhood. A tumor-suppressor gene, *WT1*, was isolated in the 11p13 chromosomal region, but deletion or mutation has been found in only 15%–20% of Wilms tumors (Huff, 1998; Nakadate et al., 2001). Loss of imprinting (LOI) of insulin-like growth factor–II (*IGF2*), a paternally expressed gene at 11p15.5, has been reported to occur in 40%–70% of tumors (Ogawa et al., 1993; Rainier et al., 1993), and it was associated with a pathological subtype that occurs in a later stage of renal development (Ravenel et al., 2001). Several studies found the type of loss of heterozygosity (LOH) on 11p that is always caused by loss of the maternal chromosome in 30%–40% of tumors investigated (Schroeder et al., 1987; Grundy et al., 1994; Nakadate et al., 2001). LOI or LOH of *IGF2* may cause overexpression of a gene that gives tumor cells a growth advantage or modifies their differentiation stage (Sakatani et al., 2005), and *IGF2* is the primary candidate for being the *WT2* gene. Cytogenetic, comparative genomic hybridization (CGH), and LOH analyses of Wilms tumors showed gain or loss of specific chromosomes or chromosomal regions, indicating that *WT1*-wild-type tumors had more genomic alterations than *WT1*-mutant-type tumors (Nakadate et al., 1999; Hing et al., 2001; Ruteshouser et al., 2005). Furthermore, association of the long arm loss of chromosome 16 (16q−) with LOI of *IGF2* in Wilms tumor was recently reported (Mummert et al., 2005). However, 16q− was found in only a small portion of the tumors with LOI investigated, and no other cytogenetic abnormalities are known to be associated with LOI in the tumors. These studies indicate that Wilms tumor is a genetically heterogeneous disease, and further

Supported by: Grant-in-Aids for Third-Term Comprehensive 10-Year Strategy for Cancer Control and Scientific Research in the Ministry of Health, Labor, and Welfare of Japan.

*Correspondence to: Yasuhiko Kaneko, Division of Cancer Diagnosis, Research Institute for Clinical Oncology, Saitama Cancer Center, Ina, Saitama, Japan. E-mail: kaneko@cancer-c.pref.saitama.jp

Received 23 August 2005; Accepted 20 January 2006
DOI 10.1002/gcc.20321
Published online 3 March 2006 in Wiley InterScience (www.interscience.wiley.com).

studies are needed to clarify the genetic/epigenetic and cytogenetic background of the tumor.

We evaluated the *WT1* and *IGF2* status and performed chromosome and/or CGH analysis of 43 Wilms tumors, on the basis of which we classified them into 4 genetic/epigenetic groups: *WT1* abnormality, LOH of *IGF2*, LOI of *IGF2*, and retention of imprinting (ROI) of *IGF2*. We analyzed the relationship between cytogenetic and genetic/epigenetic changes and found an association of LOI of *IGF2* with 11q– and +12 and possibly also with 16q–.

MATERIALS AND METHODS

Patient Samples

Tumor samples were available from 68 Japanese infants or children ranging in age from 2 months to 8 years who underwent surgery or biopsy between August 1984 and February 2003. These samples were selected on the basis of tissue availability and were not gathered consecutively. Of the 68 patients, 21 were registered in the Japan Wilms Tumor Group Study (JWITS). Samples of normal tissue were obtained from either the peripheral blood or normal renal tissue adjacent to the tumor from the same patients. Informed consent was obtained from the parents, and the study design was approved by the ethics committee of Saitama Cancer Center. The tumors were staged according to the National Wilms' Tumor Study group (NWTS) staging system, and most patients were treated according to NWTS protocols (d'Angio et al., 1989). None of the 68 patients had a family history of Wilms tumor. One patient (275) had Drash syndrome, and another patient (953) had bilateral tumors; the remaining patients had sporadic and unilateral tumors (Table 1).

Histological Examination

In all tumors, the diagnosis of Wilms tumor was made with routine hematoxylin- and eosin-stained pathology slides by local pathologists from each institution according to the classification proposed by the Japanese Pathological Society and/or the NWTS pathology panel (Beckwith et al., 1978; Japanese Pathological Society, 1988). Twenty-one cases that were registered at the JWITS were also reviewed by the pathology panel.

Cytogenetic, Fluorescence In Situ Hybridization, and CGH Studies

Chromosomes from tumor cells were studied by methods reported previously (Nakadate et al., 1999), and karyotypes were described according to the International System of Human Cytogenetic Nomenclature (ISCN, 1995). Fluorescence in situ hybridization (FISH) using Vysis probes [CEP 3 (chromosome 3 centromere), CEP 12 (chromosome 12 centromere), CBFB (16q22), and MLL (11q23); Downers Grove, IL) were carried out as described previously (Watanabe et al., 2002). CEP 12 was used to detect trisomy 12 and CEP 3 was used as a control because chromosome and CGH analyses detected 2 copies of chromosome 3 in almost all Wilms tumors, and the CBFB and MLL probes were used to detect 16q– and 11q–, respectively. Karyotypes of 11 of the 43 tumors described in Table 1 were reported previously (Nakadate et al., 1999).

CGH analysis was performed as described previously (Kumon et al., 2000). A chromosomal region was considered overrepresented or underrepresented if the average ratio profile was above 1.25 or below 0.75, respectively.

Analyses of WT1 Abnormalities and Allelic Loss on 11p and 11q

DNA preparation and digestion and Southern blot analysis using a *WT1* cDNA probe (WT33; Call et al., 1990), PCR–single-strand conformation polymorphism (SSCP) and subsequent direct-sequencing analysis, and allelic loss analysis on 11p and 11q were performed as described previously (Nakadate et al., 2001). Whether there was allelic loss on 11p and 11q was determined by PCR using microsatellite markers of D11S922, *TH*, *IGF2*, D11S932, *PAX6*, D11S903, D11S4100, *NCAM*, D11S1885, D11S29, and D11S1364 and using the restriction fragment length polymorphism (RFLP) sites of *WT1* (Tadokoro et al., 1993). The primer sequences used for PCR were obtained from the Genome Database (http://www.gdb.org). The results of the allelic loss analysis on 11p and 11q for 21 of the 43 tumors described in Tables 1 and 2 were reported previously (Nakadate et al., 2001).

The results of the study of promoter hypermethylation of *WT1* were reported previously (Satoh et al., 2003).

Analysis of *IGF2* Allelic Expression and Loss

The *Apa*I/*Ava*II polymorphism site in exon 9 was used to evaluate allelic expression of *IGF2*. PCR with genomic DNA from normal tissue and identification of heterozygous specimens after *Ava*II and *Hin*fI digestion were performed as described previously (Watanabe et al., 2002). RT-PCR products from the tumor RNA also were

TABLE I. Clinical, Genetic, Karyotypic and CGH findings in 43 Wilms Tumors

Patients number	Age/Sex	Stage of disease	*WT1* Abnormality	Karyotype	CGH	CEP 12/CEP 3	CBFB
Tumors with *WT1* abnormalities and LOH or ROI of *IGF2* (n = 5)							
275*	1 y 0 m/F	I	Mutation in exon 8	48,XX,+3,+6	ND		
832*	9 m/F	II	Mutation in exon 2	45,XX,del(3)(p12p14),−7	ND		
949*	1 y 3 m/F	II	Promoter methylation	44,X,-X,dic r(1;11)(p3?q3?;q25?p1?),inv(9)(p11q12)c	ND		
2375	1 y 9 m/M	IV	Homozygous deletion	46,XY	N		
M289	5 y 4 m/F	II	Mutation in exon 7	ND	enh(18),dim(11p13–11q12, 19,22)		
Tumors with LOH of *IGF2* and no *WT1* abnormalities (n = 13)							
325*	1 y 6 m/M	I	None	47,XY,+8,del(14)(q22)	ND		
528*	4 y 1 m/F	II	None	56,XX,+5,+7,+7,+9,+10,+12,+13,+18,+19,+22	enh(1q,4p,7,8,9,10,12,13,18)	3/2	2
575	3 y 11 m/M	II	None	46,XY	enh(1q)		
871	1 y 4 m/F	I	None	NM	N	2/2	2
918*	4 y 6 m/M	III	None	45,X,-Y	ND		
1075	2 y 4 m//M	IV	None	NM	N		
1390	4 y 0 m/M	I	None	NM	enh(Yq)		
1570*	11 m/F	II	None	51,XX,+7,+8,+10,+12,+13,?del(16)(q22)	enh(7,12,13),dim(16q22–qter)	3/2	1
1658*	2 y 8 m/M	III	None	46,XY,der(16)t(1;16)(q21;q12)	ND		
1752	1 y 0 m/F	III	None	46,XX	N		
2488	3 m/F	I	None	46,XX	N		
M134	10 m/F	II	None	ND	enh(6q),dim(7p)		
M204	3 y 9 m/F	IV	None	ND	enh(8,9,20),dim(Y)		
Tumors with LOI of *IGF2* and no *WT1* abnormalities (n = 7)							
548	3 y 1 m/M	II	None	NM	enh(6,8,9,12)		
1206*	3 y 10 m/F	II	None	50,XX,+12,inc/11q- detected by FISH (MLL)	ND	3/2	2
1207	4 y 4 m/F	III	None	76–87 complex changes	enh(12),dim(9,10p,11q,16q,18p)		
1435*	6 y 1 m/F	III	None	53,XX,+12,inc	ND	3/2	2
1535*	3 y 8 m/F	II	None	46,XX,dup(1)(q21q25),der(11)t(1;11)(q21;q22),del(16)(q22)	enh(1q,4p15–pter),dim(11q13–qter,16q)		
M269	4 y 6 m/F	IV	None	ND	enh(7q,14q21–qter),dim(7p,X)		
M291	8 y 0 m/F	I	None	ND	enh(1q,6,9p,12,13,18q),dim(1p,11q,19)		

(Continued)

TABLE 1. Clinical, Genetic, Karyotypic and CGH findings in 43 Wilms Tumors (Continued)

Patients number	Age/Sex	Stage of disease	*WT1* Abnormality	Karyotype	CGH	CEP 12/CEP 3	CBFB
Tumors with ROI of *IGF2* and no *WT1* abnormalities (n = 18)							
884	2 m/M	III	None	46,XY	N	2/2	2
953	1 y 1 m/F	V	None	47,XX,add(2)(p25), del(7)(q11q22),+8	ND		
1371	5 m/F	IV	None	NM	N		
1420	6 m/F	Unknown	None	46,XX	N		
1879	7 m/M	I	None	46,XY	N		
2011	2 y 7 m/M	II	None	55,XY,+2,+6,+7,+8, +10,+del(12)(q23) +del(12)(q23),+13,+14	enh(1q,2,6,7q21–qter,8,10, 12pter–q23,13,15), dim(1p,18p)		
2385	1 y 4 m/F	IV	None	46,XX	N		
2677	4 y 4 m/F	II	None	46,XX	enh(2)		
2749	5 y 2 m/M	II	None	46,XY	dim(22)		
M126	2 y 5 m/F	III	None	ND	enh(2p14–pter,3q,6,7,8, 12,13,17)		
M175	1 y 9 m/F	I	None	ND	N		
M188	1 y 0 m/M	I	None	ND	N		
M196	1 y 5 m/F	III	None	ND	N		
M232	1 y 2 m/F	II	None	ND	N		
M233	5 y 3 m/F	IV	None	ND	enh(6,8)		
M238	6 m/F	I	None	ND	enh(7,8,10,12,13,17,18)		
M258	4 m/M	I	None	ND	N		
M290	2 y 1 m/M	II	None	ND	enh(1q,6,7,9,12),dim(18p,Y)		

*Karyotypes of these tumors were reported previously (Nakadate et al., 1999).
Abbreviations: NM, no mitotic cells; ND, not done; N, normal; 3/2, 3 copies of CEP 12 and 2 copies of CEP 3 detected by FISH; 2, 2 copies of CBFB detected by FISH.

TABLE 2. Allelic Status of 11p and 11q and *IGF2* Imprinting Status in *WT1*, LOH of *IGF2*, and LOI of *IGF2* Wilms Tumor Groups

	p15					p13		p11	q21–22	11q23					
	S922	*IGF2*	*IGF2-LOI*	*TH01*	S932	*PAX6*	*WT1*	S903	S4100	*NCAM*	S1855	S29	S1364	*WT1* abnormality[a]	11q-detected by CGH/ cytogenetics
Tumors with *WT1* abnormalities and LOH, LOI, or ROI of *IGF2* ($n = 5$)															
275	—	●	—	●	●	—	●	—	—	○	—	○	—	Mutation in exon 8	Not detected
832	—	—	—	●	●	●	●	—	○	○	—	—	○	Mutation in exon 2	Not detected
949	—	—	—	●	—	—	●	●	●	—	—	—	●	Promoter methylation	Not detected
M289	—	○	□	○	○	○	●	●	—	—	○	○	○	Mutation in exon 7	Not detected
2375	○	○	□	○	○	—	▲	—	○	○	—	—	○	Homozygous deletion	Not detected
Tumors with LOH of *IGF* and no *WT1* abnormalities ($n = 13$)															
325	●	—	—	—	—	—	●	—	○	○	—	○	○	None	Not detected
528	—	●	—	●	●	●	—	—	●	—	●	—	●	None	Not detected
575	●	●	—	●	●	—	○	—	○	○	—	—	○	None	Not detected
871	●	—	—	●	—	●	—	—	—	○	○	○	○	None	Not detected
918	●	—	—	—	—	○	○	○	—	—	○	○	○	None	Not detected
1075	—	—	—	●	●	—	○	○	○	○	○	—	○	None	Not detected
1390	—	—	—	●	—	—	●	○	○	○	○	—	—	None	Not detected
1570	—	●	—	—	●	●	—	—	—	●	●	●	—	None	Not detected
1658	—	—	—	●	—	—	—	—	—	—	○	○	—	None	Not detected
1752	●	—	—	●	●	—	●	●	—	—	—	○	○	None	Not detected
2488	●	—	—	—	●	●	●	—	○	—	○	○	○	None	Not detected
M134	—	●	—	—	●	●	●	●	○	○	○	○	—	None	Not detected
M204	—	—	—	—	●	●	●	—	—	●	—	—	○	None	Not detected
Tumors with LOI of *IGF2* and no *WT1* abnormalities ($n = 7$)															
548	—	○	■	○	○	—	○	—	○	—	—	○	○	None	Not detected
1206	—	○	■	○	○	○	○	○	○	—	—	●	●	None	Detected
1207	—	○	■	○	—	—	—	○	—	—	—	—	●	None	Detected
1435	—	○	■	—	—	○	○	—	○	○	—	○	○	None	Not detected
1535	○	○	■	○	—	—	○	—	—	●	●	●	—	None	Detected
M269	○	○	■	○	○	○	○	○	○	—	—	○	○	None	Not detected
M291	○	—	■	○	—	○	○	—	●	—	●	●	●	None	Detected

[a]Details of *WT1* abnormality are described in the text.
● Loss of heterozygosity; ○ Retention of heterozygosity; — Not informative; ■ Loss of *IGF2* imprinting; □ Retention of *IGF2* imprinting; ▲ Homozygous *WT1* deletion.

digested with *Ava*II and *Hinf*I, and allelic expression of *IGF2* was determined.

Statistical Analysis

The significance of differences in various clinical and cytogenetic aspects of the disease among the 4 genetic/epigenetic groups of tumors was determined by the chi-square or Fisher's exact tests. Differences in the mean age of the patients and in the average number of chromosome changes between any 2 of the 4 groups were examined with Welch's *t* test.

RESULTS

Allelic Loss on 11p and 11q

Allelic loss on 11p and 11q was analyzed in Wilms tumor samples from 68 patients. Informative 11p15 loci were found in normal tissue from 64 of the patients; the 11p15 loci in the tissue from the other 4 patients were uninformative. Of the 64 informative tumors, 16 showed LOH. Of the 48 tumors without LOH, 27 were informative for the *Apa*I/*Ava*II polymorphism site of the *IGF2* gene. Thus, 43 tumor samples were the subject of the present study.

Three tumors (949, 528, and 1570) showed LOH for the entire chromosome 11; 1 tumor (M204) showed LOH on 11p15–11q23, retaining heterozygosity in the more distal 11q locus; 3 tumors (575, 918, and 1075) showed LOH limited to the 11p15 region; and 9 (275, 832, 325, 871, 1390, 1658, 1752, 2488, and M134) showed LOH limited to the 11p15–11p13 region (Table 2). Of the 27 tumors without LOH on 11p15, 1 (M289) showed

LOH limited to 11p13–11p11, and 4 (C1206, C1207, C1535, and M291) showed LOH on 11q (Table 2).

WT1 Abnormalities

Of the 9 tumors with LOH limited to the 11p15–11p13 region, 2 showed a *WT1* mutation; one (275) had a missense mutation in exon 8 (G to A conversion in nucleotide 1064; Haber et al., 1991), and the other (832) had a nonsense mutation (C to T conversion in nucleotide 550) in exon 2 (Table 2). Another tumor (C949) was found to have *WT1* promoter methylation, which was examined in 21 of the 43 tumors, of which only 1 showed the methylation (Satoh et al., 2003). This tumor had a ring chromosome containing chromosomes 1 and 11. Because the incidence of promoter methylation was quite low, and no other tumors showed a ring chromosome containing chromosome 11 and LOH for the entire chromosome 11, the other 22 tumors whose *WT1* promoter methylation status was not examined were assumed to be unmethylated.

Of 27 tumors without LOH on 11p15, 1 (M289) with LOH limited to the 11p13–11p11 region had a missense mutation in exon 7 (G to T conversion in nucleotide 895), and another (C2375) with retention of heterozygosity (ROH) for the entire chromosome 11 had homozygous deletion of the 6.6-kb fragment of *WT1*, detected by Southern blotting with a *WT1* cDNA probe and *Eco*RI digestion (Call et al., 1990; Table 2).

LOI of *IGF2*

Of the 27 tumors with ROH in 11p15 and the informative *Apa*I/*Ava*II polymorphism site of *IGF2*, 7 showed LOI of *IGF2* (Tables 1 and 2, Fig. 1). Of the 20 ROI tumors, 2 (M289 and C2375) showed *WT1* abnormalities as described before.

Four Groups of Tumors Classified by *WT1* and *IGF2* Status

We classified 43 Wilms tumors into 4 groups on the basis of major genetic abnormalities: *WT1* abnormality, LOH of *IGF2*, LOI of *IGF2*, and tumors without *WT1* or *IGF2* abnormalities. Three tumors with a *WT1* abnormality and LOH on 11p15–11p13 were included in the *WT1* group because *WT1* abnormalities are believed to have a stronger impact on tumorigenicity than LOH of *IGF2*. Thus, of the 43 tumors, 5 were classified into the *WT1* group, 13 into the LOH group, 7 into the LOI group, and 18 into the ROI group (Table 1).

CGH patterns and/or karyotypes were available for all 43 tumors (Table 1). Four tumors (528, 1206, 1435, and 1570) with a hyperdiploid karyotype (≥50 chromosomes) and trisomy 12 with or without other changes were also studied by FISH using the CEP 3, CEP 12, and CBFB probes. All 4 tumors were shown to have trisomy 12, and 1 was shown to have 16q−. One tumor (1206) was shown to have 11q− using FISH with the *MLL* probe.

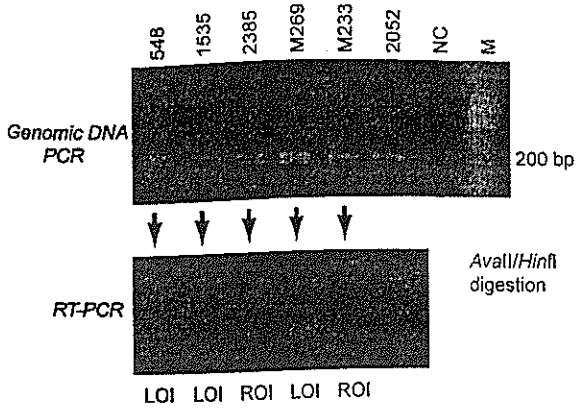

Figure 1. Electrophoretic patterns of products of genomic DNA PCR or reverse-transcription PCR after AvaII and HinfI digestion. Normal tissue from samples 548, 1535, 2385, M269, and M233 was observed to have heterozygous *IGF2* alleles, and normal tissue from sample 2052 was observed to have homozygous *IGF2* alleles, in upper lanes; loss of imprinting was found in tumor tissue from samples 548, 1535, and M269 and retention of imprinting in tumor tissue from samples 2385 and M233, in lower lanes [NC, negative control (H_2O); M, size marker].

Clinical Characteristics of Patients in Each Tumor Group

The mean age of the patients was higher in the LOI group than in the *WT1* ($P = 0.03$), the LOH ($P = 0.01$), the ROI ($P < 0.01$), or the *WT1* + LOH + ROI ($P < 0.01$) groups (Table 3). There were no differences in stage distribution among the 4 groups. The tumors of 42 patients were classified as having a favorable histology, and the tumor of 1 patient (1390) was classified as having unfavorable histology (the diffuse anaplasia type). Of the 43 patients, 41 were alive with no evidence of disease at the last follow-up (November 30, 2004). Two patients had died: the patient who had the diffuse anaplasia–type tumor died of the disease, and the patient in the *WT1* group who had Drash syndrome (275) died of renal failure.

Association of Chromosome Abnormalities with *IGF2* and *WT1* Status

Ten chromosome/CGH abnormalities were seen in 4 or more tumors (Table 3). Loss limited to 11q was more frequent in the LOI group than in the *WT1* ($P = 0.08$), the LOH ($P < 0.01$), the ROI ($P < 0.01$), or the *WT1* + LOH + ROI ($P < 0.01$)

TABLE 3. Relationship between Cytogenetic Abnormalities with 4 Wilms Tumor Groups Classified by *WT1* or *IGF2* Status

Tumors classified by *WT1* and *IFG2* status	Number of tumors	Mean age of patients in months (range)	Mean number of cytogenetic changes	+1q	+6	+7/+7q	7p-	+8	+10	11q-[a]	+12[b]	+13	16q-[c]
A. Tumors with *WT1* abnormalities and LOH or ROI of *IGF2*	5	24.2 (9–64)	0.4	0	1	0	1	0	0	0	0	0	0
B. Tumors with LOH of *IGF2* and no *WT1* abnormalities	13	28.7 (3–54)	1.5	3	1	2	1	4	2	0	2	2	2
C. Tumors with LOI of *IGF2* and no *WT1* abnormalities	7	57.4 (37–96)	2.7	2	2	1	1	1	0	4	5	1	2
D. Tumors with ROI of *IGF2* and no *WT1* abnormalities	18	23.2 (2–63)	1.3	2	4	4	0	6	2	0	4	3	0

Mean age: C versus A, $P = 0.03$; C versus B, $P = 0.01$; C versus D, $P < 0.01$; C versus A+B+D, $P < 0.01$.
Mean number of cytogenetic changes: A versus B, $P = 0.12$; A versus C, $P < 0.01$; A versus D, $P = 0.13$; A versus B+C+D, $P < 0.01$.
[a]11q-: C versus A, $P = 0.08$; C versus B, $P < 0.01$; C versus D, $P < 0.01$; C versus A+B+D, $P < 0.01$; C versus A (2 tumors with ROI)+D, $P < 0.01$.
[b]+12: C versus A, $P = 0.03$; C versus B, $P = 0.02$; C versus D, $P = 0.06$; C versus A+B+D, $P < 0.01$; C versus A (2 tumors with ROI)+D, $P = 0.02$.
[c]16q-: C versus A, $P = 0.46$; C versus B, $P = 0.6$; C versus D, $P = 0.06$; C versus A+B+D, $P = 0.12$; C versus A (2 tumors with ROI)+D, $P = 0.06$.

groups. When we added 4 tumors with LOH in the entire chromosome 11 or in the 11p15–11q23 region to the 11q− category, 11q− was still more frequent in the LOI group than in the *WT1*+LOH+ROI group ($P = 0.02$).

Trisomy 12 was more frequent in the LOI group than in the *WT1* ($P = 0.03$), LOH ($P = 0.02$), ROI ($P = 0.06$), or LOH+ROI+*WT1* ($P < 0.01$) groups. Loss of 16q was found only in the LOI or the LOH group, but there was no significant difference among the 4 groups, or between the LOI and the *WT1*+LOH+ROI groups ($P = 0.12$). Mummert et al. (2005) excluded tumors with LOH on 11p15 in a correlation analysis of 16q− and LOI of *IGF2* because LOI of the maternal *IGF2* allele prior to its deletion could not be ascertained. When we excluded 16 tumors with LOH on 11p15, 16q− tended to be more frequent in the LOI group than in the *WT1* group with the ROI of *IGF2* + ROI group ($P = 0.06$). No other associations between chromosome abnormalities with any of the 4 groups were found (Fig. 2).

For the 10 chromosome/CGH abnormalities observed in 4 or more tumors, the mean number per tumor was lower in the *WT1* group (0.4/tumor) than in the LOH (1.5/tumor; $P = 0.12$), LOI (2.7/tumor; $P < 0.01$), ROI (1.3/tumor; $P = 0.13$), or LOH+LOI+ROI (1.7/tumor; $P < 0.01$) groups (Table 3).

DISCUSSION

Wilms tumor is a heterogeneous disease showing various genetic/epigenetic abnormalities, including mutations/deletions of the *WT1* gene, LOH or LOI of the *IGF2* gene, and *CTNNB1* mutations frequently associated with *WT1* abnormalities (Ogawa et al., 1993; Rainier et al., 1993; Koesters et al., 1999; Mati et al., 2000; Ravenel et al., 2001). In addition, we previously reported that hyperdiploid tumors, usually including trisomy 12, might be a unique subgroup of tumors with no *WT1* abnormalities (Nakadate et al., 1999). Cytogenetic, CGH, and LOH studies have found recurrent abnormalities, including gains of 1q, 2, 6, 7, 8, 10, 12, 13, and 18 and losses of 1p, 7p, 9q, 11p, 11q, 16q, and 22q (Nakadate et al., 1999; Hing et al., 2001; Ruteshouser et al., 2005). None of the previous studies simultaneously examined the status of *WT1*, LOH or LOI of *IGF2*, LOH on 11p and 11q, and all chromosome/CGH patterns. The present study showed *WT1* abnormalities, LOH of *IGF2*, LOI of *IGF2*, and ROI of *IGF2* in 12%, 30%, 16%, and 42%, respectively, of 43 Wilms tumors.

Recently, Mummert et al. (2005) reported that Wilms tumors with 16q− had expression of *CTCF* half that of expression in tumors with normal chromosomes 16 and that LOI of *IGF2* was associated with loss of 16q. The *CTCF* gene, at 16q22, codes for an insulator protein. According to Mummert et al. (2005), when less CTCF was available to bind the differentially methylated region (DMR) upstream of *H19*, access of maternal *IGF2* to an enhancer downstream of *H19* might occur. The present study confirmed that tumors with 16q− showed either LOI or LOH of *IGF2* (Yeh et al., 2002; Mummert et al., 2005) and provided support for the association of 16q− with LOI of *IGF2*. Furthermore, the present study disclosed that 11q− and +12 were more frequent in tumors with LOI than in those with LOH, ROI, or *WT1* abnormalities.

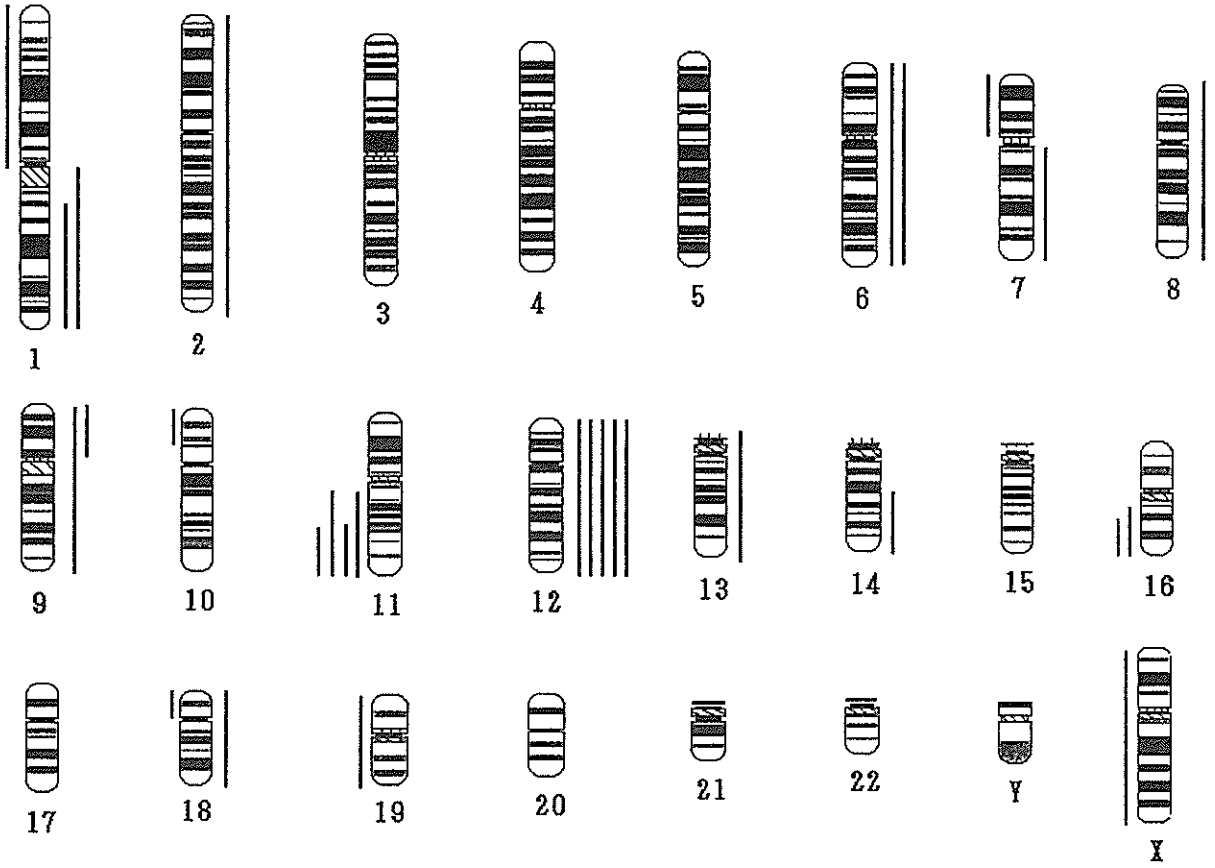

Figure 2. Summary of chromosome changes in the LOI group detected by CGH, chromosome, FISH, and/or LOH analyses. Gains and losses are shown on the right and left sides, respectively.

Overexpression of *IGF2* can be caused by LOI or by duplication of the paternal chromosome 11 with loss of the maternal chromosome 11 (LOH). LOI or LOH of *IGF2* has been detected in various embryonal tumors, including Wilms tumor, rhabdomyosarcoma, and hepatoblastoma (Ogawa et al., 1993; Rainier et al., 1993, 1995; Zhan et al., 1994). More recently, microdeletion of the maternal *H19* DMR was reported in a large family of people with Beckwith–Wiedemann syndrome (Prawitt et al., 2005). Although LOI of *IGF2* was found in fibroblasts from all 4 individuals with the microdeletion, 3 with a second genetic lesion (duplication of the microdeleted maternal *IGF2* locus), but not the one without it, developed Beckwith–Wiedemann syndrome and Wilms tumor. These findings suggest that LOI of *IGF2* or duplication of the paternal *IGF2* may be one of several genetic and epigenetic events that promote tumor cell proliferation.

The present study found an association of 11q– with LOI of *IGF2*. Very recently, Yuan et al. (2005) studied LOI of *IGF2* by assessing DNA methylation of the *H19* DMR and LOH by single-nucleotide polymorphism (SNP) chips in 58 sporadic Wilms tumors, 22 of which showed LOI. Partial loss of 11q and loss of whole chromosome 11 were found in 6 and 0, respectively, of the 22 LOI tumors, and in 1 and 13, respectively, of the 36 non-LOI tumors. They stated that 11q– was not associated with LOI. When we added 4 tumors with LOH for the entire chromosome 11 or the 11p and 11q regions into the 11q– category in the present series, 11q– was still more frequent in the LOI group than in the *WT1* + LOH + ROI group. Whole loss of chromosome 11 may play a role in loss of the wild-type *WT1* allele or in loss of the maternal *IGF2* allele, and 11q– may be a bystander in tumors with whole loss of chromosome 11 and *WT1* mutation or duplication of the paternal *IGF2* (LOH). When the 13 tumors with loss of the entire chromosome 11 from the series reported by Yuan et al. (2005) were excluded, partial loss of 11q was more frequent in the LOI tumors (6 of 22 tumors) than in the non-LOI tumors (1 of 23 tumors), $P < 0.01$, Fisher's exact

test. Thus, the present study and that of Yuan et al. (2005) lead to the same conclusion: chromosomal loss limited to 11q is associated with LOI of *IGF2* in Wilms tumor.

It has been hypothesized that 11q harbors a tumor-suppressor gene involved in the development of Wilms tumor (Radice et al., 1995; Nakadate et al., 2001). The association between 11q− and LOI of *IGF2* found in the present study suggests that Wilms tumors with overexpression of *IGF2* require deletion/mutation of the putative 11q gene in order to develop to full-blown tumors. As we have shown (Tables 1 and 2, Fig. 2), the present CGH and cytogenetic study detected physical loss of 11q DNA, rather than mitotic recombination, in the 4 tumors with LOI and 11q LOH. The gene on 11q may code for one of the proteins that constitute a CTCF insulator complex, and mutation, deletion, or haploinsufficiency of the gene may cause insulator abnormalities that might lead to LOI of *IGF2* (Ohlsson et al., 2001).

The present study also found an association between trisomy 12 and LOI of *IGF2*. We previously proposed that hyperdiploid tumors (≥50 chromosomes) make up a unique subgroup of Wilms tumors characterized by the absence of *WT1* abnormalities and nonrandom gains of chromosomes, usually including trisomy 12 (Nakadate et al., 1999). The present study added another characteristic, namely, the tendency to show LOI of *IGF2*, to the list of characteristics of hyperdiploid tumors. *CCND2* and *CDK4*, which are growth-promoting genes on chromosome 12, are overexpressed in Wilms tumors (Faussillon et al., 2005), and it is speculated that tumors with LOI of *IGF2* also need trisomy 12 in order to proliferate in an accelerated manner.

Ravenel et al. (2001) reported that patients who had Wilms tumors with LOI of *IGF2* were older than those who had tumors with normal imprinting and that the tumors with LOI were more likely to be of a pathological subtype associated with a later stage of renal development. The present study confirmed that patients with tumors with LOI were older than those who had tumors of other subtypes. Chromosome changes were most frequent in the LOI group and least frequent in the *WT1* group (Table 3). We suggest from the findings described above that tumors with LOI need far more genetic events to develop into full-blown tumors than do those with certain genetic types of tumors; it will take time to accumulate the genetic and epigenetic events that might explain why patients with LOI of *IGF2* are older.

Genes, Chromosomes & Cancer DOI 10.1002/gcc

ACKNOWLEDGMENTS

We are grateful to Dr. T. Hirama, Hokkaido Children's Medical Center (Otaru, Hokkaido); Dr. H. Mugishima, Nihon University (Itabashi-Ku, Tokyo); Dr. S. Koizumi, Kanazawa University (Kanazawa, Ishikawa); H. Kigasawa, Kanagawa Children's Medical Center (Yokahama, Kanagawa); Y. Horikoshi, Shizuoka Children's Hospital (Shizuoka, Shizuoka); T. Matsubayashi, Seirei Hamamatsu Hospital (Hamamatsu, Shizuoka); Dr. K. Kato, Nagoya First Red Cross Hospital (Nagoya, Aichi), Dr. S. Ohta, Shiga Medical College (Ohtsu, Shiga); Dr. M. Miyake, Osaka Medical College (Takatsuki, Osaka); and Dr. Y. Ishida, Ehime University (Shigenobu, Ehime) for providing samples and clinical data.

REFERENCES

Beckwith JB, Palmer NF. 1978. Histopathology and prognosis of Wilms tumor: results from the First National Wilms' Tumor Study. Cancer 41:1937–1948.

Call KM, Glaser T, Ito CY, Buckler AJ, Pelletier J, Haber DA, Rose EA, Kral A, Yeger H, Lewis WH, Jones C, Housman DE. 1990. Isolation and characterization of a zinc finger polypeptide gene at the human chromosome 11 Wilms' tumor locus. Cell 60:509–520.

D'Angio GJ, Breslow N, Beckwith JB, Evans A, Baum H, deLorimier A, Fernbach D, Hrabovsky E, Jones B, Kelalis P, Othersen B, Tefft M, Thomas PRM. 1989. Treatment of Wilms' tumor. Results of the Third National Wilms' Tumor Study. Cancer 64:349–360.

Faussillon M, Monnier L, Junien C, Jeanpierre C. 2005. Frequent overexpression of cyclin D2/cyclin-dependent kinase 4 in Wilms' tumor. Cancer Lett 221:67–75.

Grundy PE, Telzerow PE, Breslow N, Moksness J, Huff V, Paterson MC. 1994. Loss of heterozygosity for chromosomes 16q and 1p in Wilms' tumors predicts an adverse outcome. Cancer Res 54:2331–2333.

Japanese Pathological Society. 1988. Committee on histological classification of childhood tumors: tumors of the urinary system. Kanahara Shuppan, Tokyo.

Haber DA, Sohn RL, Buckler AJ, Pelletier J, Call KM, Housman DE. 1991. Alternative splicing and genomic structure of the Wilms tumor gene WT1. Proc Nat Acad Sci USA 88:9618–9622.

Hing S, Lu YJ, Summersgill B, King-Underwood L, Nicholson J, Grundy P, Grundy R, Gessler M, Shipley J, Pritchard-Jones K. 2001. Gain of 1q is associated with adverse outcome in favorable histology Wilms' tumors. Am J Pathol 158:393–398.

Huff V. 1998. Wilms tumor genetics. Am J Med Genet 79:260–267.

Koesters R, Ridder R, Kopp-Schneider A, Betts D, Adams V, Niggli F, Briner J. 1999. Mutational activation of the beta-catenin proto-oncogene is a common event in the development of Wilms' tumors. Cancer Res 59:3880–3882.

Kumon K, Kobayashi H, Namiki T, Tsunematsu Y, Miyauchi J, Kikuta A, Horikoshi Y, Komada Y, Hatae Y, Eguchi H, Kaneko Y. 2001. Frequent increase of DNA copy number in the 2q24 chromosomal region and its association with a poor clinical outcome in hepatoblastoma: cytogenetic and comparative genomic hybridization analysis. Jpn J Cancer Res 92:854–862.

Maiti S, Alam R, Amos CI, Huff V. 2000. Frequent association of beta-catenin and WT1 mutations in Wilms tumors. Cancer Res 60:6288–6292.

Mummert SK, Lobanenkov VA, Feinberg AP. 2005. Association of chromosome arm 16q loss with loss of imprinting of insulin-like growth factor–II in Wilms tumor. Genes Chromosomes Cancer 43:155–161.

Nakadate H, Tsuchiya T, Maseki N, Hatae Y, Tsunematsu Y, Horikoshi Y, Ishida Y, Kikuta A, Eguchi H, Endo M, Miyake M, Sakurai M, Kaneko Y. 1999. Correlation of chromosome abnormalities with presence or absence of WT1 deletions/mutations in Wilms tumor. Genes Chromosomes Cancer 25:26–32.

Nakadate H, Yokomori K, Watanabe N, Tsuchiya T, Namiki T, Kobayshi H, Suita S, Tsunematsu Y, Horikoshi Y, Hatae Y, Endo M, Komada Y, Eguchi H, Toyoda Y, Kikuta A, Kobayashi R, Kaneko Y. 2001. Mutations/deletions of the WT1 gene, loss of heterozygosity on chromosome arms 11p and 11q, chromosome ploidy and histology in Wilms' tumors in Japan. Int J Cancer 94:396–400.

Ogawa O, Eccles MR, Szeto J, McNoe LA, Yun K, Maw MA, Smith PJ, Reeve AE. 1993. Relaxation of insulin-like growth factor II gene imprinting implicated in Wilms' tumour. Nature 62:749–751.

Ohlsson R, Renkawitz R, Lobanenkov V. 2001. CTCF is a uniquely versatile transcription regulator linked to epigenetics and disease. Trends Genet 17:520–527.

Prawitt D, Enklaar T, Gartner-Rupprecht B, Spangenberg C, Oswald M, Lausch E, Schmidtke P, Reutzel D, Fees S, Lucito R, Korzon M, Brozek I, Limon J, Housman DE, Pelletier J, Zabel B. 2005. Microdeletion of target sites for insulator protein CTCF in a chromosome 11p15 imprinting center in Beckwith–Wiedemann syndrome and Wilms' tumor. Proc Natl Acad Sci USA 102:4085–4090.

Radice P, Perotti D, De Benedetti V, Mondini P, Radice MT, Pilotti S, Luksch R, Fossati Bellani F, Pierotti MA. 1995. Allelotyping in Wilms tumors identifies a putative third tumor suppressor gene on chromosome 11. Genomics 27:497–501.

Rainier S, Dobry CJ, Feinberg AP. 1995. Loss of imprinting in hepatoblastoma. Cancer Res 55:1836–1838.

Rainier S, Johnson LA, Dobry CJ, Ping AJ, Grundy PE, Feinberg AP. 1993. Relaxation of imprint genes in human cancer. Nature 362:747–749.

Ravenel JD, Broman KW, Perlman EJ, Niemitz EL, Jayawardena TM, Bell DW, Haber DA, Uejima H, Feinberg AP. 2001. Loss of imprinting of insulin-like growth factor–II (IGF2) gene in distinguishing specific biologic subtypes of Wilms tumor. J Natl Cancer Inst 93:1698–1703.

Ruteshouser EC, Hendrickson BW, Colella S, Krahe R, Pinto L, Huff V. 2005. Genome-wide loss of heterozygosity analysis of WT1-wild-type and WT1-mutant Wilms tumors. Genes Chromosomes Cancer 43:172–180.

Sakatani T, Kaneda A, Iacobuzio-Donahue CA, Carter MG, de Boom Witzel S, Okano H, Ko MS, Ohlsson R, Longo DL, Feinberg AP. 2005. Loss of imprinting of Igf2 alters intestinal maturation and tumorigenesis in mice. Science 307:1976–1978.

Satoh Y, Nakagawachi T, Nakadate H, Kaneko Y, Masaki Z, Mukai T, Soejima H. 2003. Significant reduction of WT1 gene expression, possibly due to epigenetic alteration in Wilms' tumor. J Biochem 133:303–308.

Schroeder WT, Chao LY, Dao DD, Strong LC, Pathak S, Riccardi V, Lewis WH, Saunders GF. 1987. Nonrandom loss of maternal chromosome 11 alleles in Wilms tumors. Am J Hum Genet 40:413–420.

Tadokoro K, Oki N, Sakai A, Fujii H, Ohshima A, Nagafuchi S, Inoue T, Yamada M. PCR detection of 9 polymorphisms in the WT1 gene. 1993. Hum Mol Genet 2:2205–2206.

Watanabe N, Kobayashi H, Hirama T, Kikuta A, Koizumi S, Tsuru T, Kaneko Y. 2002. Cryptic t(12;15)(p13;q26) producing the ETV6–NTRK3 fusion gene and no loss of IGF2 imprinting in congenital mesoblastic nephroma with trisomy 11: fluorescence in situ hybridization and IGF2 allelic expression analysis. Cancer Genet Cytogenet 136:10–16.

Yeh A, Wei M, Golub SB, Yamashiro DJ, Murty VV, Tycko B. 2002. Chromosome arm 16q in Wilms tumors: unbalanced chromosomal translocations, loss of heterozygosity, and assessment of the CTCF gene. Genes Chromosomes Cancer 35:156–163.

Yuan E, Li CM, Yamashiro DJ, Kandel J, Thacker H, Murty VV, Tycko B. 2005. Genomic profiling maps loss of heterozygosity and defines the timing and stage dependence of epigenetic and genetic events in Wilms' tumors. Mol Cancer Res 3:493–502.

ELSEVIER

EXPERIMENTAL HEMATOLOGY

Experimental Hematology 34 (2006) 508–518

Involvement of insulin-like growth factor-I and insulin-like growth factor binding proteins in pro–B-cell development

Tomoko Taguchi[a,b], Hisami Takenouchi[a], Jun Matsui[a], Wei-Ran Tang[a], Mitsuko Itagaki[a], Yusuke Shiozawa[a], Kyoko Suzuki[a], Sachi Sakaguchi[a], Yohko U. Ktagiri[a], Takao Takahashi[b], Hajime Okita[a], Junichiro Fujimoto[a], and Nobutaka Kiyokawa[a]

[a]*Department of Developmental Biology, National Research Institute for Child Health and Development, Setagaya-ku, Tokyo;* [b]*Department of Pediatrics, Keio University, School of Medicine, Shinjuku-ku, Tokyo, Japan*

(Received 14 March 2005; revised 12 December 2005; accepted 12 January 2006)

Objective. **Insulin-like growth factor (IGF)-binding proteins (IGFBPs) are a family of proteins thought to modulate IGF function. By employing an in vitro culture system of human hematopoietic stem cells cocultured with murine bone marrow stromal cells, we examined the effects of IGF-I and IGFBPs on early B-cell development.**

Materials and Methods. **Human CD34$^+$ bone marrow cells were cocultured with murine stromal MS-5 cells for 4 weeks, and pro–B-cell number was analyzed by flow cytometry. After administration of reagents that are supposed to modulate IGF-I or IGFBP function to the culture, the effect on pro–B-cell development was examined.**

Results. **After cultivation for 4 weeks, effective induction of pro–B-cell proliferation was observed. Experiments using several distinct factors, all of which neutralize IGF-I function, revealed that impairment of IGF-I function results in a significant reduction in pro–B-cell development from CD34$^+$ cells. In addition, when the effect of recombinant proteins of IGFBPs and antibodies against IGFBPs were tested, IGFBP-3 was found to inhibit pro–B-cell development, while IGFBP-6 was required for pro–B-cell development.**

Conclusions. **IGF-I is essential for development of bone marrow CD34$^+$ cells into pro-B cells. Moreover, IGFBPs are likely involved in regulation of pro–B-cell development.** © **2006 International Society for Experimental Hematology. Published by Elsevier Inc.**

Insulin-like growth factor-I (IGF-I) is an anabolic hormone and, like growth hormone and insulin, regulates whole body growth, metabolism, tissue repair, and cell survival [1]. In addition to its main production by the liver, IGF-I is also produced by bone marrow (BM) stromal cells, myeloid cells, and peripheral lymphocytes. In plasma and most biological fluids, IGF-I binds to members of a family of six specific soluble proteins, known as IGF-binding proteins (IGFBPs) 1–6, all of which have structures that are unrelated to those of IGF receptors (IGFRs) [2]. Although IGFBPs were originally described as passive circulating transport proteins, they are now recognized as playing a variety of roles in circulation, the extracellular environment, and inside the cell [3,4].

Offprint requests to: Tomoko Taguchi, M.D., Ph.D., Department of Developmental Biology, National Research Institute for Child Health and Development, 2-10-1, Okura, Setagaya-ku, Tokyo 154-8535, Japan; E-mail: ttaguchi@nch.go.jp

Of the six IGFBPs, IGFBP-3 is the most abundant IGFBP in plasma. In vitro experiments examining the effects of IGFBP-3 on various cell cultures have provided conflicting data, with both enhancement and inhibition of IGF-I actions, depending upon the cell type and culture conditions used [3,4]. In contrast, IGFBP-6 was purified from human cerebrospinal fluid and from transformed human fibroblast cell culture [3]. IGFBP-6 has been shown to inhibit IGF actions, including proliferation, differentiation, cell adhesion, and colony formation of osteoblasts and myoblasts [4]. Although the IGFBPs differ in their structure and binding specificity, functional differences among the various IGFBPs are still not clear [4].

In view of its multiple effects, IGF-I is thought to play an integral role in hematopoiesis [1]. IGF-I stimulates growth of bones and seems to control the volume of BM, thereby regulating production of hematopoietic cells [5]. Moreover, IGF-I has been suggested to have direct effects on development of a variety of hematopoietic cells. In the case of

0301-472X/06 $–see front matter.
doi: 10.1016/j.exphem.2006.01.009

B-cell development in mice, for example, previous reports have indicated that IGF-I stimulates maturation of pro-B cells into pre-B cells [6] and acts as a B-cell proliferation cofactor to synergize with the activity of interleukin (IL)-7 [7]. Indeed, administration of IGF-I increased the number of pre-B cells in BM and splenic B cells in normal mice and after BM transplantation [8]. However, the effect of IGF-I on B-cell development, especially in humans, is still largely unknown. In addition, although murine BM stromal cells secrete IGFBPs, the functional role of them in hematopoiesis remains unclear.

In an attempt to clarify the effect of IGF-I and IGFBPs on early B-cell development, we employed an in vitro culture system of human hematopoietic stem cells (HPSCs) cocultured with murine BM stromal cells that induce pro-B cells. In this article, we expand upon results of previous reports by other authors [6–8] and show that IGF-I is essential for pro–B-cell induction from HPSCs. In addition, we also report that IGFBP-3 inhibits pro–B-cell development, whereas IGFBP-6 is required for pro–B-cell development. The possible role of IGFBPs in early B-cell development is discussed.

Materials and methods

Reagents

Recombinant human and mouse IGF-I, IGFBPs, and the IGF-IR kinase inhibitor I-OMe-AG538 were obtained from PeproTech EC Ltd. (London, UK), G-T Research Products (Minneapolis, MN, USA), and Calbiochem-Novabiochem Co. (San Diego, CA, USA), respectively. All reagents are solved in phosphate-buffered saline, except I-Ome-AG538, which is solved in dimethyl sulfoxide, and diluted to the indicated concentration by culture medium.

The following mouse monoclonal antibodies (mAbs) against human antigens were used: anti-IGF-IR from G-T; purified anti-CD19, fluorescein isothiocyanate (FITC)-conjugated anti-μ heavy chain, and phycoerythrin (PE)-conjugated anti-κ and anti-λ light chains and anti-CD25 from Becton Dickinson Biosciences (San Diego, CA, USA); FITC-conjugated anti-CD24, CD43, and CD45, PE-conjugated anti-CD10, CD20, CD33, and CD179a, and PE-cyanine (PC)-5–conjugated anti-CD19 from Beckman/Coulter Inc. (Westbrook, MA, USA). The CD179a molecule, also known as VpreB, is a component of surrogate light chain and is specifically expressed in B-cell precursors, including pro-B and pre-B cells, but not in mature B cells [9]. Hamster mAb against mouse IGF-I and goat polyclonal anti-mouse IGF-I, and IGFBPs Abs were obtained from G-T. Rabbit polyclonal Abs against human IGF-IR and phosphospecific IGF-IR were purchased from Cell Signaling Technology (Beverly, MA, USA). Goat polyclonal anti–β-actin Ab was obtained from Santa Cruz Biotechnology, Inc. (Santa Cruz, CA, USA). Secondary Abs were obtained from Molecular Probes, Inc. (Eugene, OR, USA), and Dako Cytomation, Co. (Glostrup, Denmark), respectively. All other chemical reagents were obtained from Wako Pure Chemical Industries, Ltd. (Osaka, Japan), unless otherwise indicated.

Cells and cultures

Human BM $CD34^+$ cells purchased from Cambrex Bio Science Walkersville, Inc. (Walkersville, MD, USA) were used. These cells had been isolated from human tissue after obtaining informed consent. A cloned murine BM stromal cell line, MS-5, was kindly provided by Dr. A. Manabe (St. Luke's International Hospital, Tokyo, Japan) and Dr. K. J. Mori (Nigata University, Nigata, Japan). Human B-precursor acute lymphoblastic leukemia cell line NALM-16 was kindly provided by Dr. Y. Matsuo (Grand Saule Immuno research Laboratory, Nara, Japan) and was maintained in RPMI-1640 supplemented with 10% (v/v) fetal calf serum (FCS; Sigma-Aldrich Fine Chemical Co., St. Louis, MO, USA) at 37°C in a humidified 5% CO_2 atmosphere.

For induction of pro-B cells, MS-5 cells were plated at a concentration of 1×10^5 cells on a 12-well tissue plate (Asahi Techno Glass Co., Chiba, Japan). The next day, 4×10^4 cells/well/2 mL $CD34^+$ cells were plated onto the MS-5 cells in culture medium supplemented with 10% FCS and various combinations of reagents, as indicated in the figures. Because our preliminary experiments revealed that cultures in an RPMI-1640 medium produced a higher yield of B cells compared with cultures in α-minimum essential medium (data not shown), we used RPMI-1640 medium for the following experiments. After cultivation for the indicated periods, cells were harvested using 0.25% trypsin plus 0.02% ethylenediamine tetraacetic acid (IBL Co. Ltd., Gunma, Japan), and the number of cells per well was determined. All experiments were performed in triplicate, and means ± standard deviations (SD) of cell numbers are shown in Figures 1C, 3, 4, 5C, and 5D. For the histology studies, cells were cultured on type-I collagen-coated cover slips (Asahi Techno Glass) and were examined by May-Grünwald-Giemsa staining or immunohistochemical staining.

Immunofluorescence study

A multicolor immunofluorescence study was performed using a combination of FITC, PE, and PC-5. Cells were stained with fluorescence-labeled mAbs and analyzed by flow cytometry (EPICS-XL, Beckman/Coulter), as described previously [10]. Staining of the cytoplasmic antigens was performed using Cytofix/Cytoperm Kits (Becton Dickinson), according to manufacturer's protocol. To detect surface immunoglobulin $(Ig)^+$ mature B cells and cytoplasmic μ^+ pre-B cells simultaneously, cells were first stained with a mixture of PC-5-conjugated anti-CD19 Ab and PE-conjugated Abs against κ/λ light chains and then treated with cell permeabilization reagents followed by staining of cytoplasmic antigens. It was confirmed by preliminary experiments that permeabilization treatment does not affect the signals of surface antigens stained beforehand. For cell sorting, human BM $CD34^+$ cells cocultured with MS-5 for 4 weeks were harvested and stained with PC-5–conjugated anti-CD19 mAb. $CD19^+$ cells were sorted in an EPICS-ALTRA cell sorter (Beckman/Coulter). For CD19 immunostaining, cover slips were fixed with ice-cold acetone for 15 minutes and stained with anti-CD19 mAb and examined by confocal laser scanning microscope (FV500; Olympus, Tokyo, Japan) as described previously [11].

RT-PCR, immunoblotting, and detection of IGF-I

Total RNA was extracted from cultured cells, and reverse transcriptase polymerase chain reaction (RT-PCR) was performed as described previously [12]. The sets of primers used in this study are listed in Table 1. Cell lysates were prepared by solubilizing the cells in lysis buffer and immunoblotting was performed as described previously [13]. The concentration of mouse IGF-I in